# Effects of distributed transmission speeds on propagating activity in neural populations

Axel Hutt*
*Humboldt University at Berlin, 12489 Berlin, Germany*

Fatihcan M. Atay†
*Max Planck Institute for Mathematics in the Sciences, 04103 Leipzig, Germany*

(Received 11 September 2005; revised manuscript received 5 January 2006; published 14 February 2006)

Motivated by experimental evidence, a distribution of axonal transmission speeds is introduced into a standard field model of neural populations. The resulting field dynamics is analytically studied by a systematic investigation of the stability and bifurcations of equilibrium solutions. Using a perturbation approach, the effect of distributed speeds on bifurcations of equilibria are determined for general connectivity and speed distributions. In addition, a nonlinear analysis of traveling fronts is given. It is shown that the variance of the speed distribution affects the frequency of bifurcating periodic solutions and the phase speed of traveling waves. Moreover, a new effect is discovered where the introduction of axonal speed distributions leads to the maximization of the traveling front speed.

DOI: 10.1103/PhysRevE.73.021906 PACS number(s): 87.18.Hf, 02.60.Nm, 87.19.La

The measured activity of the neural system indicates that the spatiotemporal dynamics of the brain is intimately related to the various brain functions and cognition. As examples we mention the space-time instabilities during several types of hallucinations [1] and epileptic seizures [2]. Hence, the study of the dynamics of neural models is important for understanding neural and cognitive processes. In recent years, several models of coupled neurons have attracted much attention, including networks involving spatial structures [3–8], describing a continuous, synaptically coupled neural field extended in space. The dynamics of these fields is governed by integro-differential equations. In addition, the finite signal transmission speed along the axons results in a space-dependent delay between two distant locations; i.e., the neural field shows a retarded interaction [9]. Recent works have modeled this delay by using a finite value $v$ for axonal transmission speed [5,10,11] or two different values of $v$ for excitatory and inhibitory connections [12,13]. On the other hand, the propagation speed along the axon depends on a number of factors, such as its myelination.[1] The natural diversity in the degree of myelination of the axons leads to a diversity in the propagation speeds. Indeed, experimental studies reveal not a single axonal speed but statistically distributed speeds in cortico-cortical connections in rats [9] and in intracortical connections in the visual cortex of cats and monkeys [14,15]. In these studies, the histogram of axonal speeds fits a $\gamma$ distribution with maxima between 5 m/s and 12 m/s in rats and at about 0.2 m/s in the cat and monkey brains. To our best knowledge, such distributions of propagation speeds have not yet been considered in dynamical neural models.[2] Motivated by physiological and experimental evidence, in this paper we introduce a distribution of signal transmission speeds into the classical field model of neural dynamics. We present an analytical investigation of the effects of distributed speeds on the dynamics through the stability of equilibria, the bifurcations leading to spatial patterns and oscillations, and properties of traveling fronts.

An important ingredient of neural activity is the input-output behavior of synapses which convert incoming pulses to postsynaptic potentials. In the coarse-grained population model, at time $t$ and some point $x$ in the field, ensembles of excitatory and inhibitory chemical synapses respond to incoming pulse activity, yielding an effective postsynaptic potential $V(x,t)$. In classical models of a homogeneous field, the dynamics of $V$ can be described by [5]

$$\frac{\partial}{\partial t}V(x,t) + V(x,t) = \bar{\alpha}\int_{\Omega} K(|x-y|)S(V(y,t-|x-y|/v))dy + I(x,t).$$

Here $\Omega$ is the spatial domain, which we take to be the one-dimensional line in the subsequent analysis. The kernel $K$ gives the spatial distribution for excitatory and inhibitory synaptic connections. The nonlinear transfer function $S$ represents the ensemble pulse activity generated by the effective membrane potential [16] and is monotone increasing. For unimodally distributed firing thresholds of the neurons in the population, $S$ is typically taken to have a sigmoidal shape [12]. Furthermore, $I$ is the external stimulus, $\bar{\alpha}$ represents the synaptic efficacy, and $v$ is the transmission speed along axons between the population neurons. A detailed review of the derivation of the basic model can be found in Ref. [12]. In

*Electronic address: axel.hutt@physik.hu-berlin.de
†Electronic address: atay@member.ams.org, URL: http://personal-homepages.mis.mpg.de/fatay

[1]The myelin is a fatty material, composed chiefly of lipids and lipoproteins, that encloses certain axons and nerve fibers and affects their electrical conductance.

[2]Nunez [9] considers distributed speeds in an integral equation model, similar to Eq. (1) but without a temporal differentiation operator.

 

this paper, we extend previous studies of neural populations by assuming a statistical distribution of axonal transmission speeds and thus introduce a speed distribution $g(v)$ into the above model to obtain

$$\frac{\partial}{\partial t}V(x,t)+V(x,t)=\bar{\alpha}\int g(v)\int_{-\infty}^{\infty}K(|x-y|)\times S(V(y,t-|z|/v))dydv+I(x,t). \quad (1)$$

Here, $g$ is an arbitrary probability density function—i.e., $g(v)\geqslant 0$ and $\int g(v)dv=1$. Furthermore, from physical considerations we stipulate that $g$ is zero outside of some interval $(v_l,v_h)$, where $v_l$ and $v_h$ are positive numbers denoting, respectively, the lower and upper bounds of biologically possible transmission speeds.

We first determine the equilibrium solutions and their stability. For a constant input $I(x,t)\equiv E^*$, a spatially uniform equilibrium solution $V(x,t)\equiv V^*$ of Eq. (1) satisfies the equation

$$V^*=S(V^*)\bar{\alpha}\int_{-\infty}^{\infty}K(z)dz+E^*, \quad (2)$$

which may have one or more solutions $V^*$. The stability of $V^*$ is determined by the linear variational equation

$$\frac{\partial}{\partial t}u(x,t)+u(x,t)=\alpha\int g(v)\int_{-\infty}^{\infty}K(z)u(x+z,t-|z|/v)dzdv, \quad (3)$$

where $u(x,t)=V(x,t)-V^*$ and

$$\alpha=\bar{\alpha}S'(V^*)\geqslant 0. \quad (4)$$

Note that by Eq. (4), the value of the external input $E^*$ affects $\alpha$ through the value of $V^*$ as the solution of Eq. (2). Using the ansatz $u(x,t)=e^{\lambda t}e^{ikx}$ in Eq. (3), where $\lambda\in\mathbb{C}$ and $k\in\mathbb{R}$, we obtain the dispersion relation between the temporal and spatial modes as

$$\lambda+1=\alpha\int_{v_l}^{v_h}g(v)\int_{-\infty}^{\infty}K(z)e^{-\lambda|z|/v}e^{-ikz}dzdv. \quad (5)$$

Since the eigenvalues of the operator $L=\partial/\partial t+1$ given by the left-hand side of Eq. (3) have negative real parts, $V^*$ is asymptotically stable for $\alpha=0$ and thus also for small $\alpha$. If $\alpha$ increases further, the stability of the equilibrium solution can be lost as an eigenvalue $\lambda$ crosses the imaginary axis. At the critical transition there is an eigenvalue $\lambda=i\omega$, with $\omega\in\mathbb{R}$, and the bifurcating solutions can be qualitatively classified as stationary or oscillatory depending on whether $\omega=0$ or $\omega\neq 0$, respectively, and as spatially homogeneous or inhomogeneous depending on whether $k=0$ or $k\neq 0$, respectively. It can be shown that stationary bifurcations are independent of the delays introduced by finite propagation speeds, whereas the delays turn out to be important in oscillatory bifurcations [11,12].

The study of oscillatory bifurcations is clearly important because of the prevalence of oscillatory activity in neural systems. For instance, a spatially homogeneous and oscillatory bifurcation ($\omega\neq 0$ and $k=0$) corresponds to spatially uniform, or synchronous, oscillations, whereas the spatially inhomogeneous case ($\omega\neq 0$ and $k\neq 0$) corresponds to traveling waves, with wave speed given by $\omega/k$. The analysis of these bifurcations by solving Eq. (5) is not straightforward. To obtain results applicable for general connectivity and speed distributions, we introduce the power series expansion

$$u(x+z,t-|z|/v)=\sum_{m=0}^{\infty}\frac{(-|z|/v)^m}{m!}\frac{\partial^m}{\partial t^m}u(x+z,t)$$

into Eq. (3). The infinite series can be truncated to yield an approximation for the dynamics, and the error committed will be small when the transmission speeds are sufficiently large and the connection kernel $K$ decays sufficiently fast [11]. For the reduced equation obtained by neglecting terms of order $N+1$ and higher, the relation (5) has the form of a polynomial in $\lambda$:

$$\lambda+1=\alpha\sum_{m=0}^{N}\frac{(-1)^m}{m!}\lambda^m E[v^{-m}]\hat{K}_m(k),$$

where $E[v^{-m}]=\int v^{-m}g(v)dv$ is the expected value of $v^{-m}$ and $\hat{K}_m(k)=\int_{-\infty}^{\infty}|z|^m K(z)e^{-ikz}dz$ denotes the Fourier transforms of the moments of $K$. Taking $N=0$ is equivalent to neglecting all propagation delays in the field, while $N=1$ gives an equation that depends only on the mean value of propagation speeds and not their distribution. Thus, the lowest-order approximation that retains the effects of distributed speeds is obtained by taking $N=2$. For this case, the dispersion relation (5) reduces to a quadratic equation in $\lambda$:

$$p_k(\lambda)=c_2(k)\lambda^2+c_1(k)\lambda+c_0(k)=0, \quad (6)$$

with coefficients

$$c_0(k)=1-\alpha\hat{K}_0(k),$$

$$c_1(k)=1+\alpha E[v^{-1}]\hat{K}_1(k),$$

$$c_2(k)=-\frac{1}{2}\alpha E[v^{-2}]\hat{K}_2(k).$$

The analysis of Eq. (6) gives qualitative information about the behavior of the full dispersion relation (5) at nearby parameter values.

The bifurcation conditions can now be determined. For stationary bifurcations, we see that the pair $(\lambda,k)$ with $\lambda=0$ satisfies Eq. (6) if and only if

$$\alpha\hat{K}_0(k)=1. \quad (7)$$

For oscillatory bifurcations, the pair $(\lambda,k)$ with $\lambda=i\omega$, $\omega>0$, satisfies Eq. (6) if and only if

$$\alpha E[v^{-1}]\hat{K}_1(k)=-1 \quad (8)$$

and

$$\omega^2=2\frac{\alpha\hat{K}_0(k)-1}{\alpha E[v^{-2}]\hat{K}_2(k)}>0. \quad (9)$$

As noted above, the equilibrium solution is stable for small $\alpha$, since the bifurcation conditions (7) and (8) do not hold. As $\alpha$ is further increased, stability can be lost through a stationary or oscillatory bifurcation, characterized by the conditions (7)–(9), respectively. Note that the stationary bifurcation condition (7) depends only on the connectivity kernels and not on the delays. Furthermore, in case of instantaneous signal propagation ($v=\infty$), we have $E[v^{-1}]=0$, and by Eq. (8) oscillatory bifurcations cannot occur. Thus, stability can be lost through an oscillatory bifurcation only in the case of delayed signal propagation.

In order to study the effects of distributed transmission speeds on the dynamics, we keep the mean value $E[v^{-1}]$ fixed and change the variance $\mathrm{var}[v^{-1}]$. It then follows from the conditions (7) and (8) that the stability of the equilibrium solution is unaffected by the variances and the bifurcations occur at (approximately) the same parameter values. In particular, the wave number $k^*$ at bifurcation does not depend on the variance of the speed distribution. The main effect of the variances is on the frequency $\omega$ of oscillatory bifurcations, as given by Eq. (9). Since $E[v^{-2}]=\mathrm{var}[v^{-1}]+E^2[v^{-1}]$, we see that the frequency $\omega^*$ at bifurcation will decrease with increasing variance $\mathrm{var}[v^{-1}]$. In the case of bifurcating traveling waves, an increase in $\omega^*$ corresponds to an increase in the speed $\omega^*/k^*$ of the waves since $k^*$ is unaffected by the variance of speeds. Thus, the spread of the speed distribution affects the frequency of bifurcating oscillatory solutions and the phase speed of traveling waves.

To illustrate by numerical calculations, we take the spatial domain $\Omega$ to be a circle with circumference $C$ (or equivalently an interval $[0,C]$ with periodic boundary conditions). We choose $K$ to be

$$K(z)=\frac{a_e}{2}e^{-|z|}-\frac{a_i}{2}re^{-r|z|}, \tag{10}$$

where $r$ denotes the relation of excitatory and inhibitory spatial ranges and $a_e$ and $a_i$ represent excitatory and inhibitory synaptic weights. For instance, when $r>a_e/a_i$ the neural field exhibits local inhibition and lateral excitation and thus facilitates traveling waves in case of a single propagation speed [17]. The transfer function has been chosen as the logistic function $S(V)=10/\{1+\exp[-1.8(V-3.0)]\}$. The distribution of propagation speeds is described by the truncated $\gamma$ density

$$g(v)=\frac{N_{p,q}}{q^p\Gamma(p)}v^{p-1}\exp(-v/q), \quad p>2, \quad q>0, \tag{11}$$

in the speed range $0<v_l\leqslant v\leqslant v_h$, where $N_{p,q}$ is the normalization factor arising from the truncation. This choice of $g(v)$ reflects experimental findings [9,14,15]. Figure 1 shows (untruncated) $\gamma$ distributions for various $p$. The maximum of $g(v)$ occurs at $v_m=q(p-1)$; furthermore, $E[v^{-1}]=N_{p,q}/(N_{p-1,q}v_m)$ and $\mathrm{var}[v^{-1}]=N_{p,q}(p-1)/(N_{p-2,q}(p-2)v_m^2)-E^2[v^{-1}]$. We determine the phase speed $\omega/k$ of bifurcating waves from Eq. (9). In Fig. 2 the resulting phase speed is plotted with respect to $v_m$ and $\mathrm{var}[v^{-1}]$. It can be seen that the phase speed is lower than $v_m$ and grows roughly linearly with $v_m$. This relation of the front speed and the transmission speed is similar to previous findings for single transmission speeds [11,17,18]. In addition, we see here that increasing the variance decreases the phase speed of the waves; that is, the broader the speed distribution, the lower the resulting phase speed for bifurcating waves.

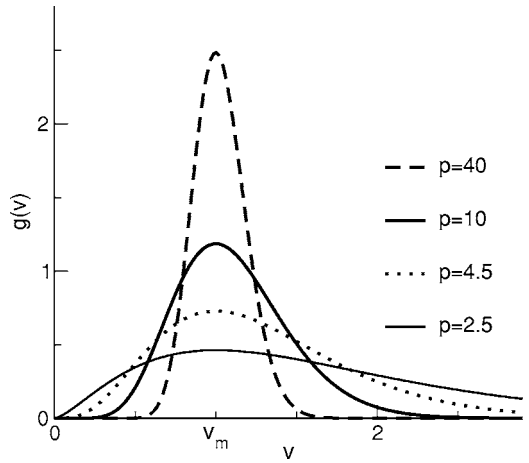


FIG. 1. $\gamma$-distributed transmission speeds.

The preceding results were derived using a linear analysis of bifurcations of spatially uniform equilibrium solutions and are valid for high transmission speeds. We now relax this constraint and turn to a direct analysis of traveling fronts to study the effects of speed distributions. Assuming a single firing threshold $u_0$ in the neural population, the transfer function $S$ assumes the form of the Heaviside step function $\Theta$. Without loss of generality we take the external input to be zero, and the field dynamics obeys

$$\frac{\partial V(x,t)}{\partial t}+V(x,t)=\int_{v_l}^{v_h}g(v)\int_{-\infty}^{\infty}K(|x-y|)\times\Theta(V(y,t-|x-y|/v)-u_0)dydv.$$

We treat the front mathematically in a coordinate system

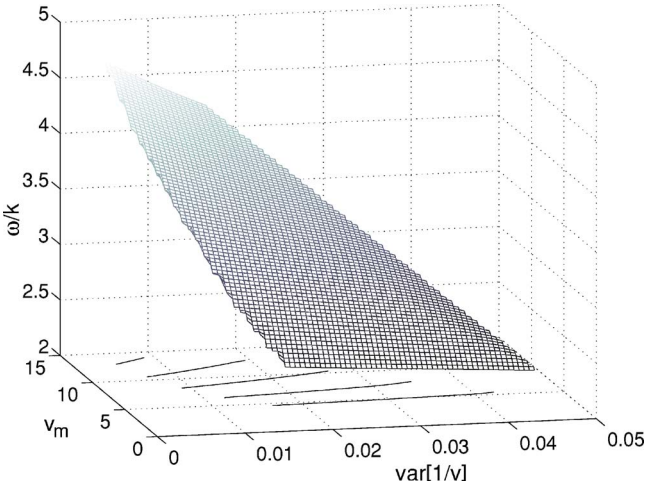


FIG. 2. (Color online) The propagation speed of bifurcating traveling waves. Contour lines of the speed are plotted on the bottom horizontal plane to help visualization. Parameter values are $r=3$, $a_e=100$, $a_i=99$, $v_l=4$, $v_h=100$, and $\alpha=2.0$.

moving with speed $c$, writing $V(x,t)=u(x-ct)$. The boundary conditions are $\lim_{z\to-\infty}u(z)=\kappa:=\int_{-\infty}^{\infty}K(z)dz$ and $\lim_{z\to\infty}u(z)=0$; furthermore, the field is fixed at $u(0)=u_0$. This results in an ordinary differential equation in $u(z)$, and the usual considerations to ensure a finite solution yield a condition of the form

$$h(c) := u_0 - \kappa/2 + E\left[\mathcal{L}\left(\frac{v-c}{vc}\right)\right] = 0, \tag{12}$$

where

$$E\left[\mathcal{L}\left(\frac{v-c}{vc}\right)\right] = \int g(v)\int_0^{\infty}\exp(-z/c)\gamma K(\gamma z)dzdv$$

is the mean value of a Laplace transform, with $\gamma=v/(v-c)$. For the specific choices (10) and (11), this condition reads

$$\kappa/2 - u_0 = \frac{N_{p,q}}{2q^p\Gamma(p)}\int_{v_l}^{v_h} v^p\exp(-v/q) \times\left(\frac{a_e}{v-c+vc} - \frac{a_i r}{v-c+vcr}\right)dv.$$

Equation (12) determines the front speed $c$ implicitly. For the particular parameters chosen, a unique value of $c$ was numerically observed; however, in general Eq. (12) may show multiple solutions. Figure 3 shows the solutions of $h(c)=0$—i.e., the resulting front speed—with respect to the peak $v_m$ and the variance var$[1/v]$ of the speed distribution. Recall that the distribution parameter $q$ is fixed to $q=v_m/(p-1)$. We first observe the saturation of the front speed $c$ for large transmission speeds and low variances—i.e., for narrow speed distributions. This result shows accordance with previous results obtained for a single transmission speed [10]. Moreover, broad distributions—i.e., larger variances—yield a maximum front speed at specific values of $v_m$. Subsequently, there is an optimal variance of transmission speeds which maximizes the speed of traveling fronts. To our best knowledge, this effect has not been found before and sheds new light on delayed interactions in nonlocal neural systems.

To summarize, we have introduced transmission speed distributions to the standard neural population model and studied their effects on the oscillatory solutions and traveling fronts of neural fields. The relation between the connectivities and delays plays a significant role in the analysis. We have presented an approximation scheme which gives qualitative information about the bifurcation structure and has the advantage of being applicable to rather arbitrary field connectivities and speed distributions when the mean speed is high. Furthermore, we have given a nonlinear analysis of traveling wave fronts which is valid for any range of mean speeds and does not depend on local bifurcation conditions. The results show that the shape of the speed distribution affects the speed of traveling waves and the oscillation frequency of synchronous activity. In particular, the presence of broad speed distributions yields a local maximum for front speeds. This result may indicate an optimization procedure in nature, whereby the information transfer is maximized by distributed axonal transmission speeds. A detailed analysis will be presented in a forthcoming extended article.

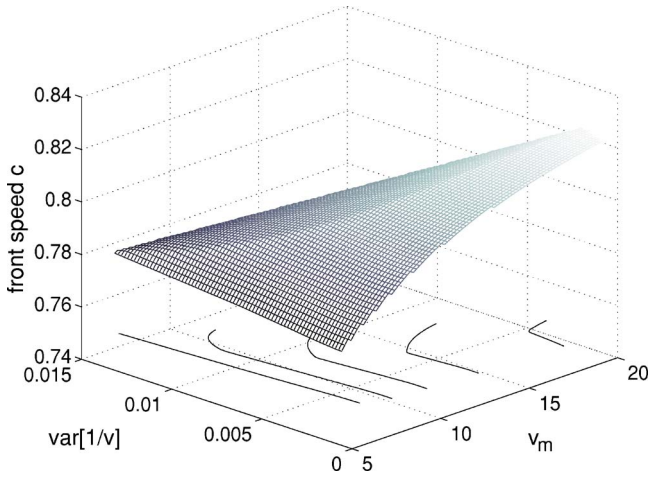


FIG. 3. (Color online) The front speed $c$ with respect to the peak $v_m$ and the variance var$[1/v]$ of the speed distribution in an excitatory field. Parameter values are $a_e=8$, $a_i=0$, $V_l=4$, $V_h=20$, $u_0=1$, and $r=0.5$.

A.H. has obtained financial support from the Deutsche Forschungsgemeinschaft (Grant No. SFB-555).

[1] J. R. Brasic, Percept. Mot. Skills **86**, 851 (1998).
[2] F. H. Lopes da Silva, W. Blanes, S. Kalitzin, J. Parra, P. Suffczynski, and D. Velis, Epilepsia **44**, 72 (2003).
[3] H. Wilson and J. Cowan, Biophys. J. **12**, 1 (1972).
[4] S. Amari, Biol. Cybern. **27**, 77 (1977).
[5] P. Bressloff and S. Coombes, Int. J. Mod. Phys. B **11**, 2343 (1997).
[6] W. Gerstner, Phys. Rev. E **51**, 738 (1995).
[7] V. Jirsa, Neuroinformatics **2**, 183 (2004).
[8] A. Hutt, Phys. Rev. E **70**, 052902 (2004).
[9] P. Nunez, *Neocortical Dynamics and Human EEG Rhythms* (Oxford University Press, New York, Oxford, 1995).
[10] D. Pinto and G. Ermentrout, SIAM J. Appl. Math. **62**, 206 (2001).
[11] F. M. Atay and A. Hutt, SIAM J. Appl. Math. **65**, 644 (2005).
[12] A. Hutt and F. M. Atay, Physica D **203**, 30 (2005).
[13] A. Hutt and F. M. Atay, Chaos Solitons Fractals (to be published).
[14] V. Bringuier, F. Chavane, L. Glaeser, and Y. Fregnac, Science **283**, 695 (1999).
[15] P. Girard, J. Hupe, and J. Bullier, J. Neurophysiol. **85**, 1328 (2001).

[16] W. Freeman, Int. J. Bifurcation Chaos Appl. Sci. Eng. **2**, 451 (1992).
[17] A. Hutt, M. Bestehorn, and T. Wennekers, Network Comput. Neural Syst. **14**, 351 (2003).
[18] S. Coombes, G. Lord, and M. Owen, Physica D **178**, 219 (2003).